Journal of Intelligent & Robotic Systems (2025) 111:99
https://doi.org/10.1007/s10846-025-02296-3

REGULAR PAPER

Radio Localization for Robotic Planetary Exploration: Lessons Learned from a Space-Analogue Mission

Robert Pöhlmann[1] · **Emanuel Staudinger**[1] · **Siwei Zhang**[1] · **Armin Dammann**[1]

Received: 3 October 2023 / Accepted: 8 July 2025

Abstract
Autonomous robotic systems will be the future of planetary exploration missions. For autonomous robotic exploration, reliable pose estimation is required. This can be provided by cooperative radio localization, where radio signals are exchanged among the robots and other mission objects. Range and direction information is obtained by measuring the signal round-trip time (RTT) and direction-of-arrival (DoA), which enables position and orientation estimation of the robots. For the first time, we have demonstrated cooperative radio localization within a space-analogue exploration mission with two robotic rovers on the volcano Mt Etna. With this paper, we share our main lessons learned based on a thorough evaluation of measurement data. Thereby we identify estimation biases as the main error source. We then show how to estimate and compensate these biases during the mission by simultaneous localization and calibration (SLAC). We further investigate the impact of the radio signals reflected on the ground and on mission objects on the ranging accuracy. Then, we demonstrate the benefit of cooperation and the feasibility of single-link localization. In addition, we share tangible ranging and DoA estimation error models based on measurements in a realistic environment.

Keywords Direction-of-arrival · Error modeling · Moon · Navigation · Simultaneous localization and calibration · Two-way ranging

1 Introduction

Autonomous robots will play an important role in future planetary exploration missions [1]. Heterogeneous teams of robots can combine the potential of e.g. ground-based and airborne robots and can collaborate to solve complex tasks [2].

To enable autonomous robotic exploration, reliable localization is essential. The pose of the robots, i.e. their positions and orientations, must be estimated and tracked over time. Knowledge of the pose is necessary to control the robots, but also e.g. to pinpoint scientific measurements and camera images.

Robotic pose estimation is often done using wheel odometry [3], visual odometry [4], inertial sensors or a combination thereof. However, when the robots travel longer distances, the pose estimation suffers from drifts due to accumulating errors. By simultaneous localization and mapping (SLAM), pose estimates can be greatly improved by detecting loop closures [5]. For loop closures, previously explored areas must be revisited. In most cases, loop closures cannot be achieved when the robots need to travel far away from the lander to a distant area of interest. Furthermore, allowing additional travel of the rovers for loop closures might not be feasible due to energy and time constraints.

For the Moon, a satellite based communication and localization system has been proposed [6] and is being considered as part of ESA's Moonlight initiative [7]. However, unlike satellite navigation on earth, the system will only consist of very few satellites, thus coverage will not be continuous and the accuracy will be limited.

✉ Robert Pöhlmann
robert.poehlmann@dlr.de

Emanuel Staudinger
emanuel.staudinger@dlr.de

Siwei Zhang
siwei.zhang@dlr.de

Armin Dammann
armin.dammann@dlr.de

[1] Institute of Communications and Navigation, German Aerospace Center (DLR), Oberpfaffenhofen, Muenchener Str. 20, 82234 Wessling, Germany

Published online: 05 September 2025

To address these shortcomings, we have developed a cooperative radio localization system for robotic pose estimation [8]. Recently in July 2022, we have demonstrated the system in a space-analogue mission on the volcano Mt Etna, Sicily, Italy, see Fig. 1.

With this paper, we provide the following contributions:

- We share our main lessons learned from the space-analogue mission regarding cooperative radio localization.
- Specifically, we investigate the bias as the major error source of ranging and direction-of-arrival (DoA) observations.
- We further show how to estimate and compensate such biases during the mission by simultaneous localization and calibration (SLAC), which considerably improves the localization accuracy. We provide comparative measurement results for cooperative and non-cooperative localization and SLAC.
- We investigate the impact of the two-ray ground reflection on the ranging accuracy and examine sources of radio signal scattering.
- We experimentally demonstrate the feasibility of single-link radio localization.
- We publish error models for ranging and DoA estimation, which can be used to simulate radio localization for exploration missions and sensor fusion.

The paper is organized as follows. We discuss related work in Section 2. Then, we introduce our cooperative radio localization system in Section 3 and the space-analogue robotic exploration mission in Section 4. The following Section 5 is dedicated to an in-depth analysis of radio localization during the analogue mission. We treat seven specific topics and break each topic down to a concise lessons learned based on our experiences. In Section 6 we present error models for ranging and DoA estimation based on the measurement data from the analogue mission. Finally, Section 7 concludes the paper.

2 Related Work

2.1 DoA and ToA Estimation

Cooperative radio localization relies on range and/or direction information extracted from radio signals. The range can be estimated from the received signal strength (RSS) using a propagation model. As this often does not match reality with sufficient accuracy, the approach is prone to errors [9]. An accurate range estimate between pairs of transceivers can be obtained from the signal round-trip time (RTT) by measuring the time-of-arrivals (ToAs) of the exchanged radio signals [10]. Using a multiport antenna, e.g. an antenna array [11] or a multi-mode antenna [12], the signal DoA can be estimated.

2.2 Cooperative Radio Localization

Localization in radio networks is an active field of research, see [13, 14] and the references therein. A general dis-

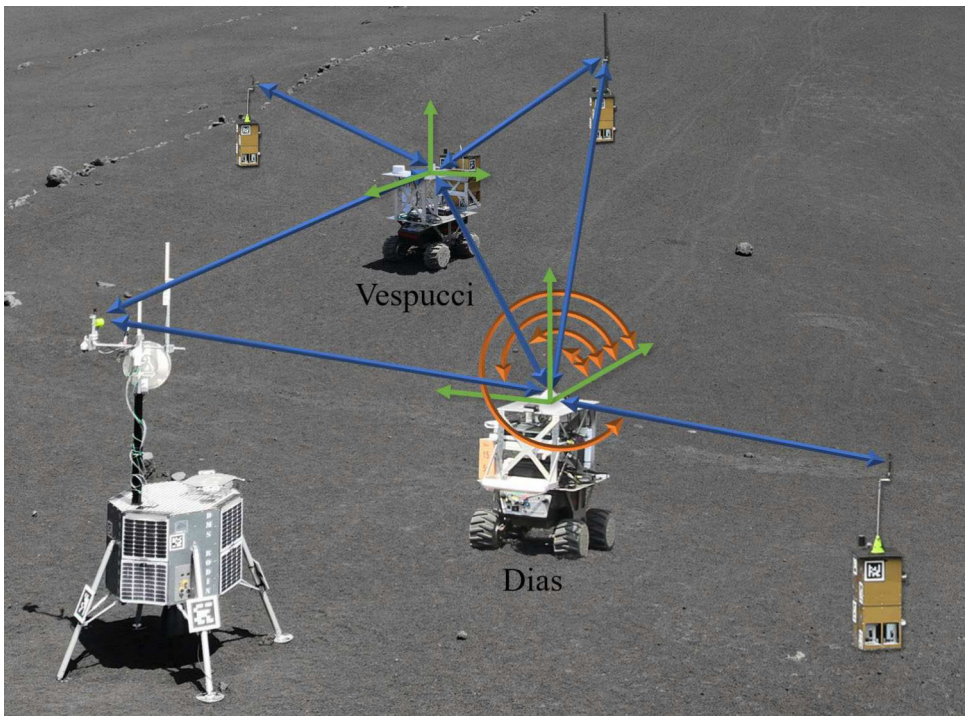

Fig. 1 Experiment setting of the space-analogue mission on Mt Etna with the lander, two rovers and multiple anchor and payload boxes. The rover's poses are highlighted in green, the ranges in blue and the DoAs in orange

tinction is between non-cooperative and cooperative radio localization. For non-cooperative localization, only static nodes with known position, called anchors, exchange radio signals with the robots. For cooperative localization, the robots also exchange radio signals among each other. Both, non-cooperative and cooperative radio localization have been analyzed using estimation theory, e.g. by deriving the Cramér-Rao bound (CRB) for deterministic parameters [15] or the Bayesian Cramér-Rao bound (BCRB) for random parameters [16]. In [17] the CRB and the BCRB for position and orientation estimation in non-cooperative networks have been derived. The position error bounds have been extended to cooperative networks in [18]. Position and orientation error bounds for cooperative networks, assuming phase synchronization among the nodes, have been derived in [19]. An extension to the case without phase synchronization is given by [20], but only non-cooperative networks are considered. The position and orientation CRB has been extended to arbitrary multiport antennas in [21]. By comparing the position and orientation error bounds of cooperative and non-cooperative localization, many papers have shown the superiority of cooperative localization [13, 18, 22, 23]. Positions and orientations are typically estimated and tracked over time by Bayesian filtering or recursive Bayesian estimation [24]. For an overview of cooperative radio localization algorithms see [14].

2.3 Measurements and Experiments

Cooperative radio localization is considered in the context of wireless sensor networks [9, 14], for urban scenarios as part of cellular networks [25, 26] and for indoor localization [22, 27]. Experiments mainly cover indoor scenarios [22, 28, 29]. We have published first results about cooperative radio localization of robots from the space-analogue mission on Mt Etna in [30, 31]. Apart from that, cooperative radio localization has not been demonstrated and thoroughly evaluated in a relevant environment for an extraterrestrial robotic exploration mission.

3 DLR's Cooperative Radio Localization System

At the German Aerospace Center (DLR), we have designed a cooperative radio localization system for planetary exploration. The system jointly provides localization and communication. It supports high update rates and high data rates, which are the requirements for planetary exploration missions [32]. To fulfill these requirements, the developed system is based on orthogonal frequency-division multiplexing (OFDM), which is used in state-of-the-art communications systems like IEEE 802.11 Wi-Fi and 4G and 5G cellular networks. For cooperative radio localization, radio signals are exchanged among all nodes in the network. To provide flexibility and avoid a central point of failure, radio channel access is provided by self-organized time-division multiple access (TDMA). The nodes are capable of measuring the signal ToA, which allows to estimate ranges between pairs of transceivers via the signal RTT.

The radio localization system is implemented as software-defined radio (SDR). For wireless communications specific details regarding signals, synchronization etc. of the system we refer to [8, 31]. The most important system parameters are stated in Table 1. For the space-analogue mission, the radio nodes have been integrated into two rovers, three anchor boxes, two payload boxes and the lander. On the rover Dias, a multi-mode antenna and a coherent multiport transceiver are installed, which in addition to ranging enable the estimation of the signal DoA [33]. The setting of the space-analogue mission including the lander, payload boxes and the rovers Dias and Vespucci together with ranges and DoAs is shown in Fig. 1. The received signals containing range and DoA information are used by a Bayesian filter together with command velocity and gyroscope to estimate the 3D poses of the robots [33]. In addition, the data including raw samples of the received signals are stored for evaluation in post-processing.

4 Space-Analogue Robotic Exploration Mission

We have performed the space-analogue exploration mission demonstrating cooperative radio localization in the frame of the Helmholtz future project ARCHES [2, 34]. The goal of ARCHES was the demonstration of technologies for future space exploration missions. A specific goal was to show the feasibility of exploration missions with a significantly higher level of autonomy compared to current missions. Thereby, the cooperation of heterogeneous teams of robots to solve complex tasks has been demonstrated [2]. The final demonstration of ARCHES took place as a space-analogue mission on the volcano Mt Etna on Sicily, Italy, in June and July 2022. The experiment area of the space-analogue mission is shown in Fig. 2. The volcanic environment presented the perfect

Table 1 DLR cooperative radio localization system parameters

Parameter	Value
Carrier frequency	1.68 GHz
Sampling rate	31.25 MHz
Occupied bandwidth	$\approx$ 28.2 MHz
TDMA schedule	100 ms
Transmit power	5 dBm

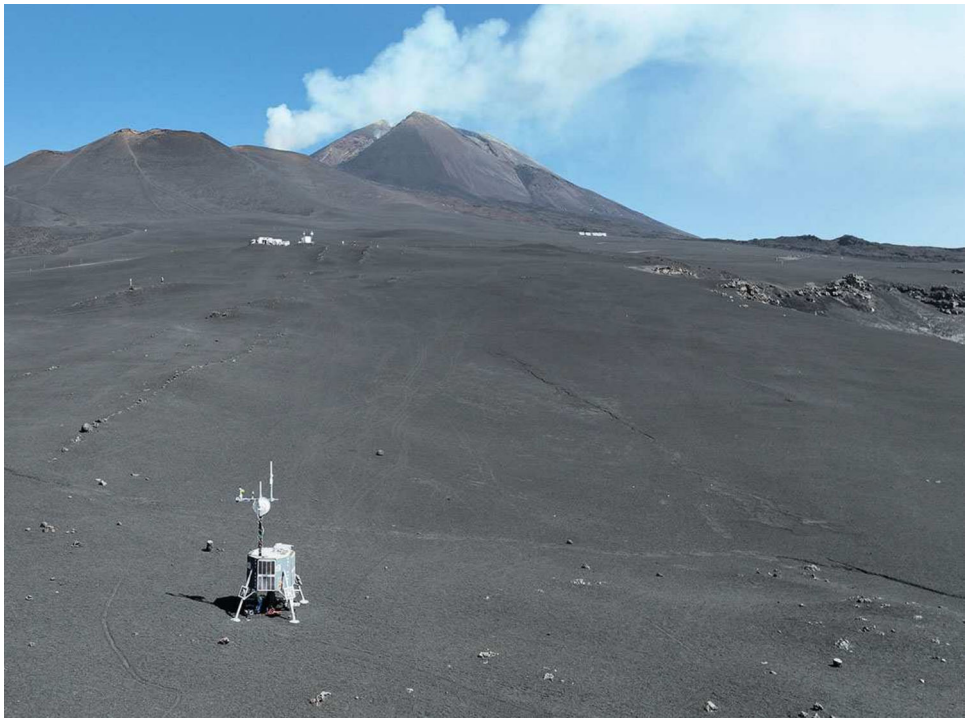

Fig. 2 Lander and experiment area of the space-analogue mission [31]

conditions for an analogue mission targeting the Moon. The lander, which had been placed beforehand, was the starting point for the robotic exploration mission.

For this paper, we focus on the space-analogue demonstration of cooperative radio localization. Figure 3 shows an aerial image of Mt Etna and the different objects involved in

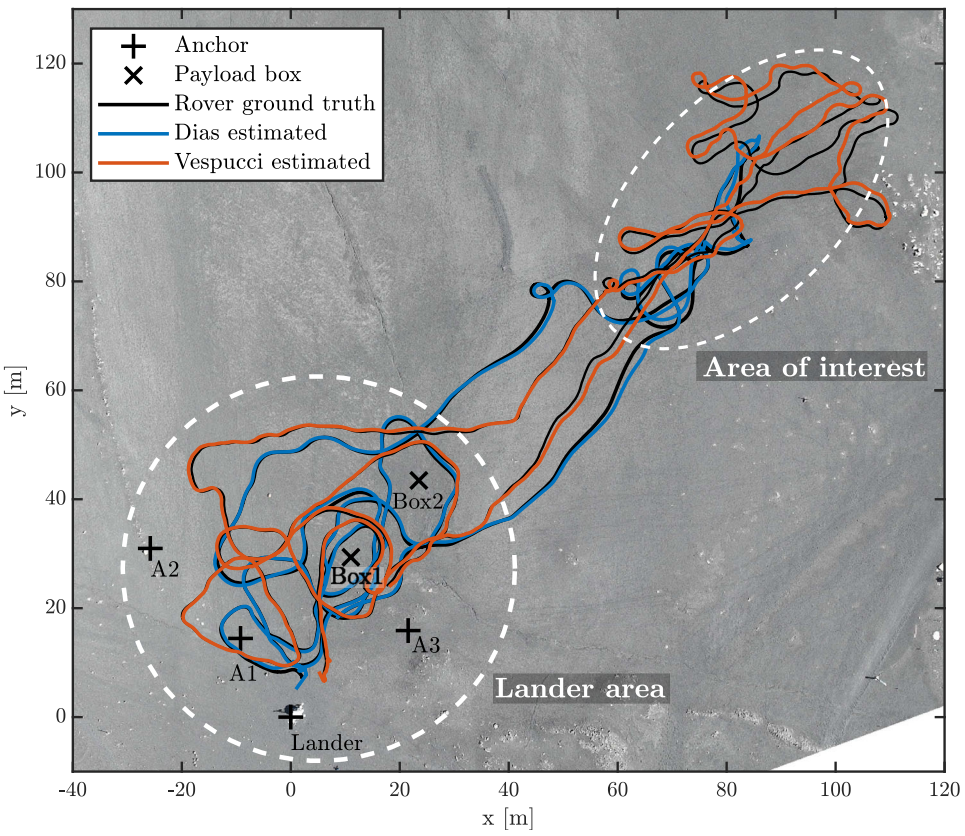

Fig. 3 Aerial image of the space-analogue mission area with anchor and payload box positions, and the ground truth and estimated trajectories for the rovers Dias and Vespucci

the mission. The positions of the anchors A1, A2, A3 and the lander were known beforehand. The positions of the payload boxes Box1 and Box2 were assumed to be unknown. The two robotic rovers Dias and Vespucci, see also Fig. 1, were equipped with a commercial two antenna real-time kinematic (RTK) and inertial system for 6D pose ground truth. The conducted experiment comprised different phases. First, the rovers drove around the neighborhood of the lander and located the two payload boxes. Meanwhile, SLAC was performed to improve the calibration of the cooperative radio localization system [33]. Then, the rovers traveled to a distant area of interest for exploration. Finally, they returned to the lander. The duration of the entire experiment was 13 min 15 s. From Fig. 3, we see that in the area between the lander, the anchors and payload boxes, the estimation is very accurate and the estimated trajectories almost perfectly match the ground truth. When the rovers travel far away to the area of interest, localization becomes more challenging due to the unfavorable geometry for localization. Thus the errors grow, but remain below a few meters. We discuss the impact of the geometry on the localization accuracy in more detail in Section 5.5.

5 Lessons Learned

In the following, we present the main results of the Mt Etna space-analogue mission regarding cooperative radio localization.

For each topic, we thoroughly analyze the measurement data. Based on that, we work out the specific problems and briefly explain the relevant background and theory, where applicable. We then break each topic down to a concise lessons learned based on our gained experiences.

5.1 Accurate Ranging Requires Bias Compensation

We start by analyzing the histogram of ranging errors for all neighbors of anchor node A3 in Fig. 4. The first thing that draws our attention is that the range estimates are biased. The bias is agent specific, considerably larger than the standard deviation (STD) and appears to be constant for the mission duration. Since RMSE $= \sqrt{\text{STD}^2 + \text{BIAS}^2}$, the ranging root-mean-square error (RMSE) is mainly dominated by the bias rather than the estimation noise.

Our results are in line with the literature. E.g. in [29, 35], ranging biases larger than the standard deviations are reported for RTT ranging measurements. The cause for these quasi-constant biases is to be found in the hardware. When radio signals propagate through the transceiver hardware, they experience group delays. When these delays are not perfectly calibrated and compensated, they cause biased range estimates. From a hardware perspective, the transceiver

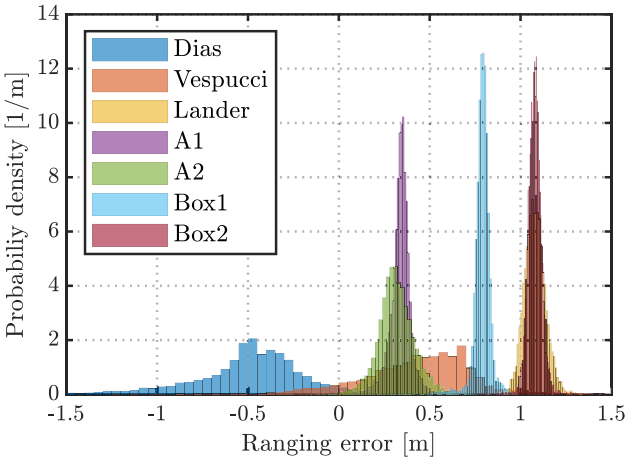

Fig. 4 Probability density histogram of the ranging errors for all neighbors of anchor node A3

should have an observation path to measure and compensate internal signal delays. Depending on the transceiver architecture, such an approach does not necessarily combat the bias entirely. Such hardware induced biases may change over time, but typically they are stable at least for a longer period, e.g. the duration of this experiment.

Investigating Fig. 4 further, we realize that the ranging error standard deviation of the two rovers is larger compared to the static nodes. The reason is twofold. First, when the rovers drive, the radio propagation environment changes. The impact of that is analyzed in the next Section 5.2. Second, in addition to the quasi-constant ranging bias, there is a direction-dependent ranging bias present. To analyze the direction-dependency of the ranging bias, we compensate the constant bias and plot the ranging error for all signals received by the rover Dias versus the signal DoA in Fig. 5. The plot reveals that the ranging error of all signals received by the rover Dias has a dependency on the DoA, which is sim-

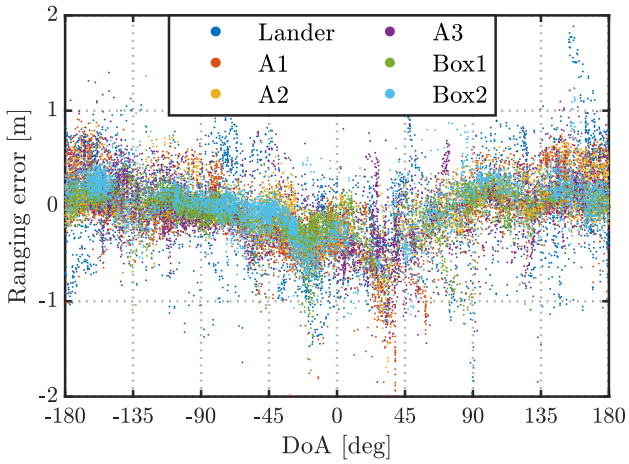

Fig. 5 Ranging error (constant bias compensated) depending on the signal DoA for all signals received by the rover Dias

ilar for all neighbors. Thus, the second ranging error source is a direction-dependent bias.

We see two reasons for the direction-dependency of the ranging error. First, more complex antennas with multiple ports like the multi-mode antenna installed on Dias often exhibit direction-dependent group delay variations. Second, anything in the nearfield of the antenna, i.e. the surrounding structure of the rover, has an impact on the antenna response and can also cause group delay variations. Both, the antenna behavior and its surroundings should be considered during the design process. Ideally, a direction-dependency can be avoided entirely.

We have identified both, quasi-constant ranging biases and direction-dependent ranging biases which deteriorate ranging accuracy. To avoid that, we have proposed the SLAC algorithm [30, 33]. By SLAC, both quasi-constant and direction-dependent ranging biases are estimated and compensated in real-time during the mission. In Fig. 6, we compare the empirical cumulative distribution functions (CDFs) of the absolute ranging error for the rovers Dias and Vespucci for standard RTT ranging and with ranging bias compensation by SLAC. The SLAC algorithm estimates and tracks localization and calibration states in a common state space. A constant ranging bias is estimated for all static nodes and a direction-dependent ranging bias is estimated for both rovers. The plot shows the effectiveness of SLAC. By SLAC, the 90th percentile ranging error for Dias and Vespucci has been reduced from 0.96 m and 1.06 m to 0.64 m and 0.62 m, respectively.

Thus, our first lesson learned is that accurate ranging requires careful compensation of ranging biases.

5.2 Two-ray Ground Reflection Decisively Impacts Ranging Accuracy

Having understood the causes of a quasi-constant and a direction-dependent ranging bias, we now investigate the distance-dependency of the ranging bias. For that, we plot the ranging error after bias compensation by SLAC versus the true range of the rover Vespucci to other agents and anchors in Fig. 7. The plot covers the entire mission duration. A range-dependent bias is clearly apparent, especially for the lander with higher antenna position over ground. Furthermore, we see fast ranging error variations for small distances and slow variations for larger distances.

The distance-dependent ranging bias is caused by radio propagation effects, specifically by the ground reflection [36]. The signal emitted by the transmitter antenna does not only travel along the direct line-of-sight path to the receiver antenna. Often there is an additional signal component which is reflected from the ground in between transmitter and receiver. Typically, the distance between transmitter and receiver is large compared to their height above ground. Thus,

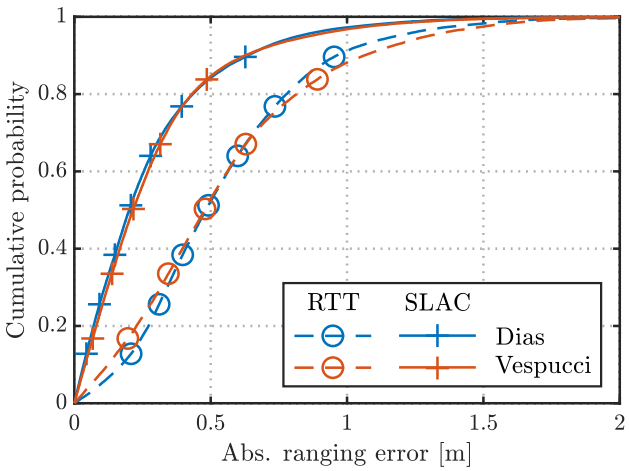

Fig. 6 Empirical CDF of the absolute ranging errors of the rovers Dias and Vespucci for standard RTT ranging and with ranging bias compensation by SLAC

the detour length of the second signal component is small. Since radio signals travel with the speed of light, the delay difference between the two signal components is so small, that it is usually not possible to separate them, even when for large signal bandwidths. Consequently, we observe a ranging bias, which is caused by the two signals overlaying constructively or destructively at the receiver depending on the detour length. The effect is well known in satellite navigation [37, 38]. In [39], a detailed theoretical analysis of the impact of the ground reflection on the ranging and radio localization accuracy for robotic planetary localization has been performed.

Assuming transmitter and receiver are at a known height above a flat ground, a theoretical model can be derived [36, 39]. Fixing antenna heights, carrier frequency and ground properties, it turns out that the ranging bias varies depending on the distance between transmitter and receiver and can

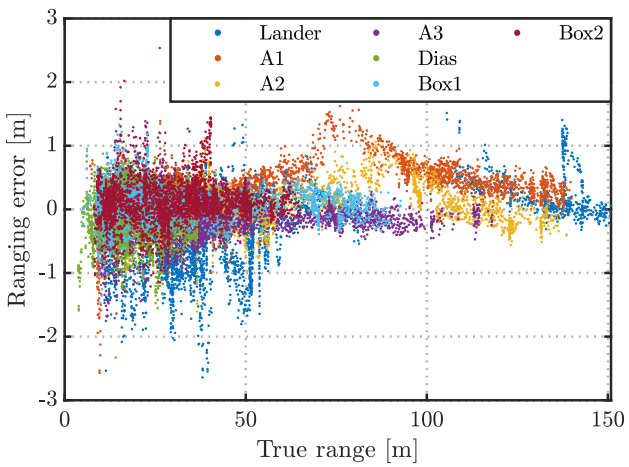

Fig. 7 Ranging error of the rover Vespucci to other anchors and agents depending on the true range. Quasi-constant agent specific and DoA-dependent ranging biases have been compensated by SLAC

be obtained by simulation. We show the main theoretical result here for clarity and refer the interested reader to [39] for a thorough treatment of the subject. Figure 8 shows the resulting ranging RMSE for different antenna heights, taking into account the system parameters of DLR's cooperative radio localization system. The plot clearly shows a strong dependency of the ranging bias on the distance. Furthermore, it also shows the impact of the antenna heights of transmitter and receiver above ground on the ranging bias. For the space-analogue mission, the antennas of the rovers and payload boxes were 0.85 m above ground. The lander antenna was 4.5 m above ground, see also Fig. 2. Furthermore, we see fast ranging RMSE variations for small distances and slow ranging RMSE variations for large distances, which is in line with a two-ray propagation model.

Thus, qualitatively the ranging error behavior is similar to Fig. 7. However, the ranging to anchor A1 and other nodes with antenna height 0.85 m shows a stronger range dependency than what would be expected from theory. While this might be surprising at first, it should be stressed that the theoretical model and Fig. 8 are only valid for perfectly flat ground. In contrast to that, the terrain of the space-analogue experiment site was hilly, see also Fig. 2. Thus, for a meaningful comparison with the theoretical two-ray ground reflection model, an accurate 3D reconstruction of the terrain would be necessary, in order to take the reflection points on the ground correctly into account. This is part of ongoing work and beyond the scope of this paper. Nevertheless, we have shown the impact of the ground reflection on the ranging error.

Hence, the second lessons learned is that considering the two-ray ground reflection is crucial when analyzing ranging accuracy for radio localization.

5.3 Accurate DoA Estimation Requires In-Situ Antenna Calibration

Next, we investigate the DoA estimation performance of the rover Dias. From the literature it is known that DoA estimation requires accurate knowledge of the antenna response, as any model mismatch leads to biased DoA estimates [40, 41]. Thus, we have calibrated the four-port multi-mode antenna installed on Dias in a nearfield measurement chamber beforehand. However, we could not fit the entire rover into the measurement chamber. Thus, the impact of the rover structure itself on the antenna response could not be measured beforehand. We apply SLAC to do an online calibration of the antenna response during localization. By that, also changes in the close vicinity of the antenna during the mission can be considered. As an example, consider a robot which is capable of grabbing and transporting payload boxes [42]. Due to the compactness of the rover, a payload box would be close to the antenna and could influence the antenna response.

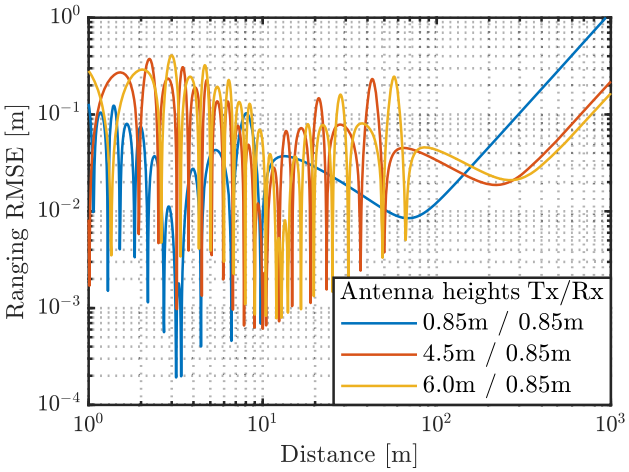

Fig. 8 Theoretical ranging RMSE versus the transmitter and receiver ground distance on a flat ground resulting from two-ray ground reflection model for different transmitter (Tx) and receiver (Rx) height combinations

The plot in Fig. 9 shows the estimated versus the true DoA of the radio signals received by the rover Dias, using two different antenna responses for the DoA estimator. Using the antenna response from the near-field measurement chamber, the estimated DoAs in general represent the true DoAs well, however for some directions estimation biases are apparent. Using the antenna response estimated by SLAC, the estimation biases are mostly compensated and the estimated DoAs are closer to the true DoAs.

The result is supported by the empirical CDF of the absolute DoA estimation error shown in Fig. 10. Using SLAC, the 90th percentile DoA estimation error is reduced from 12.4° to 8.4°. This shows the effectiveness of SLAC also for live antenna response calibration and reduction of DoA estimation biases.

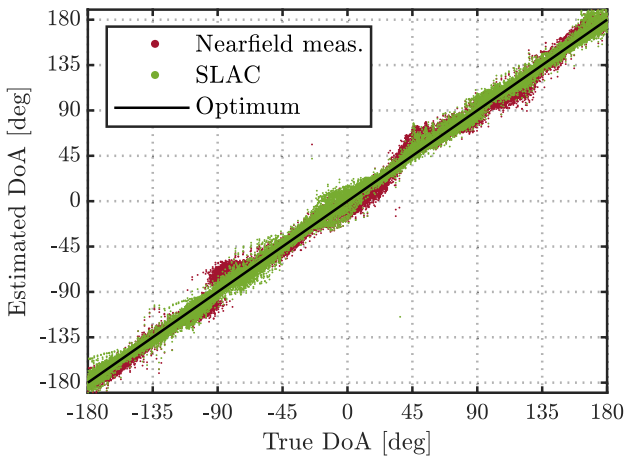

Fig. 9 Estimated versus true DoA of all signals received by the rover Dias using antenna calibration from a nearfield measurement chamber and by SLAC

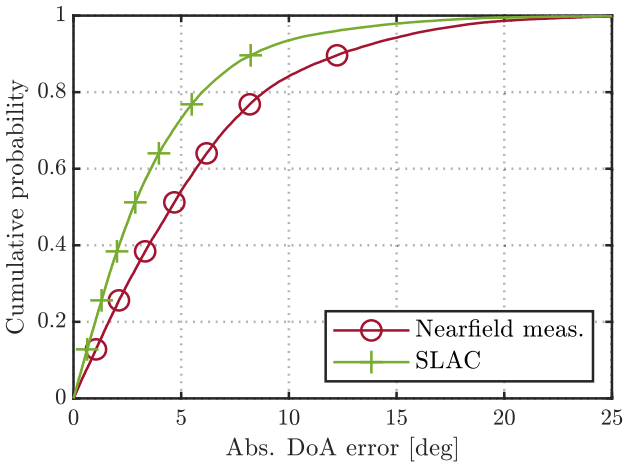

Fig. 10 Empirical CDF of the absolute DoA estimation error of all signals received by the rover Dias using antenna calibration from a nearfield measurement chamber and by SLAC

Thus, the third lesson learned is that accurate DoA estimation requires careful calibration of the antenna response, considering also the antenna surroundings, which might change during a mission.

5.4 Radio Signal Scattering On Mission Objects Should Be Avoided

At the beginning, when rovers were close to the lander, we observed that the range estimates for certain radio links were jumping between two distinct clusters of estimates several meters apart, even though the rovers were not moving. Jumping range estimates are a clear indication of multipath propagation. For further investigation, we have applied the space-alternating generalized expectation maximization (SAGE) algorithm [43, 44], which tries to separate the individual multipath components. The approach is common when analyzing radio propagation measurements for channel modeling purposes. SAGE is an iterative algorithm. Using a replica of the known transmitted signal, first the ToA, DoA and complex amplitude of the strongest multipath component is estimated. Then the strongest component is reconstructed using the estimated parameters and subtracted from the received signal. Afterwards, the parameters of the second strongest multipath components are estimated, and so on until a*the* specified or estimated number of multipath components, called model order, is reached. For the second iteration, the weaker signal components are subtracted from the received signal in order to improve the parameter estimation for the strongest component. The iterative procedure continues until convergence.

For the analysis, we fix the pose of Dias and focus on the signals received by Dias from A1. From the ranging and DoA estimates of the line-of-sight propagation path, we can determine the position of the transmitter. Locating scattering points is more complicated. To determine the location of a scattering point, we use the fact that it lies on an ellipse with transmitter and receiver in its foci [45]. The ellipse size is defined by the additional delay of the multipath component with respect to (w.r.t.) the line-of-sight path. The actual scattering point on the ellipse is then found by considering the receiver orientation and the DoA of the multipath component. For the analysis we set the model order to three, i.e. we estimate the transmitter position and two scattering points. The results are shown in Fig. 11. We see that the position estimate of A1 is ambiguous and biased due to multipath propagation. More interesting, the analysis reveals the causes of the multipath propagation. Although the estimates are biased, we can attribute the scattering points of the 2nd path to the rover Vespucci, and the scattering points of the 3rd path to the lander. Since both have metallic structures, this is not surprising. As we have observed a considerable impact of signal scattering and reflection only when the two rovers were very close to each other or to the lander, this was not a problem during the analogue missing.

Thus, radio signal scattering on mission objects is an aspect which should be taken into account for multi-agent missions. In general, there are multiple ways to tackle this issue. One solution would be to keep larger distances among the agents, hence scattered signals are much weaker than line-of-sight signals. When large distances cannot always be assured, algorithms like in [43, 44] can be applied to separate the line-of-sight from scattered signals during signal processing. The safest solution would be to attach radio frequency (RF) absorbing material to the mission objects to avoid radio signal scattering and reflections.

To summarize, the fourth lesson learned is that radio signal scattering and reflection should either be avoided by appro-

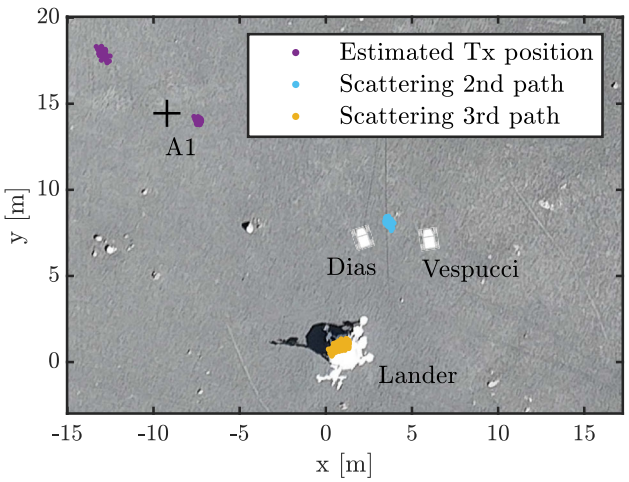

Fig. 11 Estimated transmitter (Tx) position from the line-of-sight propagation path and scattering points of the second and third multipath signal components for signals transmitted by A1 and received by the rover Dias

priate mission and hardware design or be combated by signal processing algorithms.

5.5 SLAC Outperforms Standard Localization

So far, we have done an in-depth analysis of ranging and DoA estimation. This allowed us to examine the different error sources independently, which would be difficult to separate on the localization layer. Nevertheless, in the end the position and orientation estimation accuracy are crucial for a cooperative radio localization system. Typically, positions and orientations of the robots are estimated and tracked over time by a Bayesian filter [14]. As mentioned, we propose to use SLAC, which in addition to positions and orientations also estimates calibration states. SLAC is implemented as iterated extended Kalman filter (IEKF), for details see [30, 33]. Additionally to radio signals, gyroscope measurements and the command velocity of the rovers are used for localization. In order to provide a fair comparison, we also show results for a localization-only IEKF, without calibration states.

First we investigate the position error CDFs of the rovers Dias and Vespucci shown in Fig. 12, comparing localization-only and SLAC. At about 0.85 cumulative probability, the curves are bend, which means about 15% of the position estimates have considerably higher errors compared to the rest. We attribute this behavior to the different mission phases with individual position error characteristics, which is also apparent from Fig. 3. When the rovers are in the closer vicinity of the lander and the anchors, the position errors are low. However, when the rovers travel to the distant area of interest, the position errors grow. When the rovers are far away from the lander, the resulting geometry is very challenging for radio localization. From the rover's perspective, all anchors are located far away in a similar direction. In satellite navigation, this is referred to as high dilution of precision (DOP) [38]. From Fig. 12, we see that the position error of Dias is smaller compared to Vespucci. Dias benefits from its DoA estimation capability. Also, Vespucci travels further away from the lander, such that ultimately it is connected to the network only via Dias. We analyze this challenging single-link localization scenario in Section 5.7. For both rovers, the position error with SLAC is considerably lower compared to localization-only. For Dias, the 90th percentile position error drops from 4.0 m with localization-only to 1.9 m with SLAC. For Vespucci, the 90th percentile position error is reduced from 6.1 m to 2.5 m. Thus, the ranging and DoA estimation biases are successfully estimated and compensated by SLAC.

Next, we focus on the orientation error CDFs for the two rovers shown in Fig. 13, again comparing localization-only to SLAC. In contrast to the position error, the characteristics of different mission phases are not apparent from the orientation error CDFs. As orientation estimation of the rovers is aided by gyroscopes, the orientation estimation is less sensitive to challenging geometries. Furthermore, we see that the orientation of Dias is estimated more accurately compared to Vespucci, since Dias can observe its orientation directly through the signal DoAs. We also see the improvement in orientation estimation by SLAC compared to localization-only. For Dias the 90th percentile absolute orientation error is reduced from 6.3° to 5.4° and for Vespucci from 8.5° to 7.9°. Since orientation estimation is heavily aided by gyroscopes, the improvement is smaller compared to position estimation.

Thus, as a fifth lesson learned, we conclude that SLAC outperforms localization-only for both position and orientation estimation, especially in challenging scenarios.

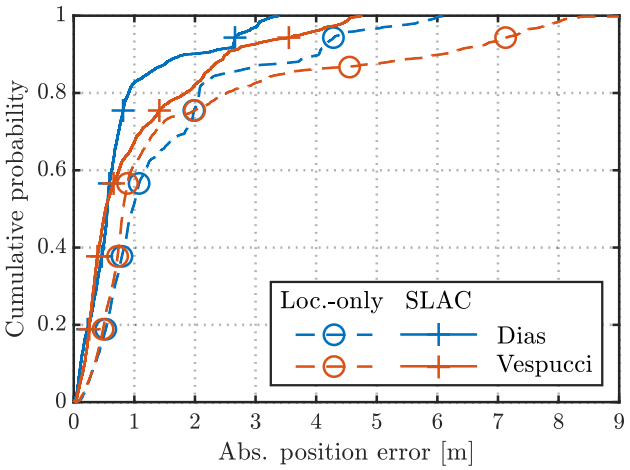

Fig. 12 Empirical CDF of the absolute position error of the rovers Dias and Vespucci for localization-only and SLAC

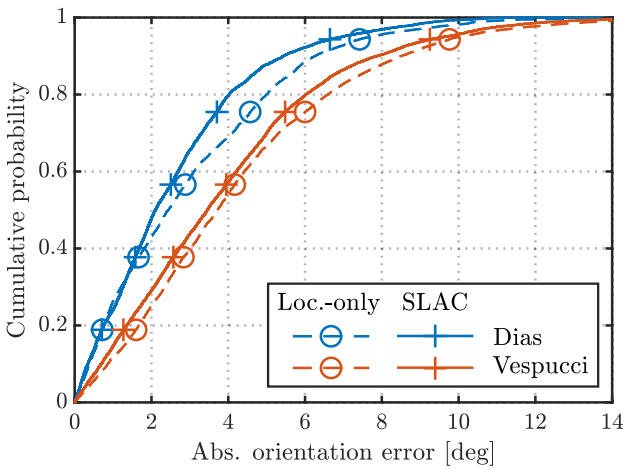

Fig. 13 Empirical CDF of the absolute orientation error of the rovers Dias and Vespucci for localization-only and SLAC

Table 2 Position RMSEs of the agents for the entire mission

Agent	Cooperative SLAC	Non-cooperative SLAC	Cooperative localization	Non-cooperative localization
Dias	1.07 m	1.21 m	2.00 m	1.46 m
Vespucci	1.50 m	2.89 m	2.78 m	3.33 m
Box 1	0.28 m	0.25 m	0.43 m	0.88 m
Box 2	0.33 m	0.57 m	0.70 m	1.06 m

5.6 Cooperation is Beneficial

Now we compare cooperative and non-cooperative radio localization approaches. Non-cooperative means that only radio signals exchanged between anchors and rovers are used for localization. Cooperative approaches use all radio signals exchanged among nodes in the network, i.e. also among rovers. We compare the position RMSEs from Table 2 and the orientation RMSEs from Table 3 for cooperative and non-cooperative localization as well as cooperative and non-cooperative SLAC. The RMSEs are calculated over the entire analogue mission, including the very challenging part where the rovers are more than 150 m away from the lander.

In accordance with Figs. 12 and 13, we see that SLAC outperforms localization-only. Furthermore, we realize that in general, cooperative outperform non-cooperative approaches. Our experimental results thus confirm theoretical results from literature [13, 18, 22, 23], which we introduced in Section 2.2. We see that for cooperative localization, the position error of one rover also affects the positioning error of the other rover. Thus, for an individual rover, the error could be larger for cooperative localization. Looking at the entire network, cooperative outperforms non-cooperative localization. Finally, with cooperative SLAC the lowest position and orientation errors are obtained, because the ranging and DoA biases can be better estimated in a cooperative fashion [33].

Hence, the sixth lesson learned is that cooperation is beneficial for radio localization.

5.7 Single-Link Localization Is Feasible

When the rover Vespucci travels far away from the lander, see Fig. 3, ultimately it is connected to the network only through the other rover Dias, which results in a challenging single-link localization scenario. Since Dias is capable of ranging and DoA estimation, Vespucci can still be localized. This situation is called single-link localization. It has been theoretically investigated in [46, 47] for cellular network localization, where a mobile user terminal is localized by a single link to a base station. For robotic planetary exploration, we extend the concept to cooperative localization and moving rovers.

In order to understand the network connectivity, we first have a look at Fig. 14. The plot shows the number of radio links for the rover Vespucci averaged over one second, corresponding to ten TDMA cycles. In the first phase, when Vespucci is close to the lander and the payload boxes, Vespucci can utilize up to seven radio links. Then, when the rovers drive away from the lander towards the area of interest, see Fig. 3, the number of available links for Vespucci decreases. Ultimately, Vespucci is so far away from the lander that it is connected to the network only via Dias. This corresponds to single-link localization. When the rovers successfully return to the lander, the number of links increases again.

To further stress the feasibility of single-link localization, we force single-link localization for Vespucci by discarding all radio signals except the ones to/from Dias for the entire experiment. The resulting position error CDF is shown in Fig. 15 in comparison to the default case, where all available radio links are used. The availability of radio links depends on the distance between the nodes and the terrain. As expected, the position error for single-link localization is larger. However, even with single-link localization, Vespucci can still be accurately localized.

As a seventh lesson learned, we consider single-link localization to be feasible.

6 Ranging and DoA Error Models

In Sections 5.1 and 5.3, we have shown the importance of ranging bias compensation and antenna calibration to reduce DoA estimation bias. Even when this is carefully done and sophisticated algorithms are applied, the resulting estimates are not perfect. They still suffer from errors, e.g. due to ther-

Table 3 Orientation RMSEs of the rovers for the entire mission

Agent	Cooperative SLAC	Non-cooperative SLAC	Cooperative localization	Non-cooperative localization
Dias	3.4°	3.8°	4.0°	3.5°
Vespucci	4.9°	5.1°	5.7°	6.7°

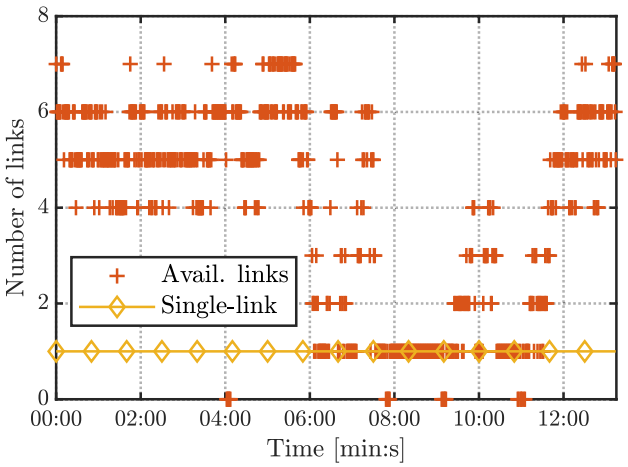

Fig. 14 Available radio links for the rover Vespucci during the space-analogue mission

mal noise in radio receivers and propagation effects discussed in Section 5.2. In addition to sharing our lessons learned from the space analogue mission, another aim of this paper is to provide tangible error models for ranging and DoA estimation. We share these error models, so they can be used by the community, e.g. to simulate exploration missions with cooperative radio localization or investigate fusion with other sensors. For sensor fusion, accurately modeling the different sensors characteristics is crucial, as model mismatch could lead to inconsistent estimates and degraded performance.

Clearly, the experienced errors depend on the system parameters, mainly transmit power, carrier frequency and signal bandwidth. The carrier frequency has an impact on the ranging bias caused by two-ray ground reflection, which we discussed in Section 5.2. Furthermore, the errors also depend on hardware properties. As we stressed in Sections 5.1 and 5.3, accurate ranging and DoA estimation requires bias compensation and in-situ calibration. Therefore, the results presented here consider ranging bias compensation and in-situ antenna calibration by SLAC. Finally, the actual environment also has an impact, e.g. the soil properties influence the strength of the ground reflection. Thus, the exact error models provided here are specific to the DLR Cooperative Radio Localization System in a Moon-analogue environment. Nevertheless, the error models provide a good impression of the performance that can be expected of a cooperative radio localization system, that has been demonstrated in robotic exploration mission in Space-analogue environment.

We use two probability distributions to model the observed errors. First, a Gaussian distribution with mean μ and standard deviation σ, which has the robability density function (pdf)

$$p(x) = \frac{1}{\sigma\sqrt{2\pi}} e^{-\frac{1}{2}\left(\frac{x-\mu}{\sigma}\right)^2}. \tag{1}$$

Second, we use a location-scale t-distribution with location μ, scale σ and shape ν with pdf

$$p(x) = \frac{\Gamma(\frac{\nu+1}{2})}{\sigma\sqrt{\nu\pi}\,\Gamma(\frac{\nu}{2})} \left(\frac{\nu + \left(\frac{x-\mu}{\sigma}\right)^2}{\nu}\right)^{-\frac{\nu+1}{2}}, \tag{2}$$

where $\Gamma(.)$ is the gamma function.

Figure 16 shows ranging error histograms for all ranging measurements of the rovers Dias and Vespucci over the entire mission duration. A very small amount of ranging errors, 0.12%, are outside of the plotted range [−2 m, 2 m]. Their practical impact is typically small, as they would usually be detected and excluded by an outlier rejection mechanism. The ranging errors of Dias and Vespucci are very similar.

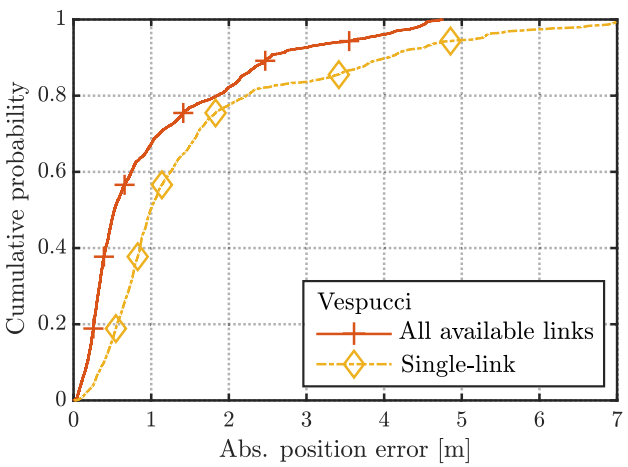

Fig. 15 Empirical CDF of the absolute position error of the rover Vespucci using all available radio links, and using only the radio link with the rover Dias to perform single-link localization

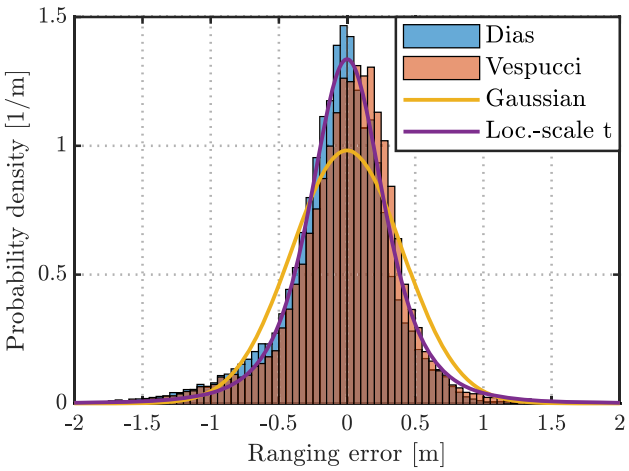

Fig. 16 Probability density histogram of the ranging errors of the rovers Dias and Vespucci, Gaussian pdf with $\mu = 0$ m, $\sigma = 0.41$ m and Location-scale t pdf with $\mu = 0$ m, $\sigma = 0.28$ m, $\nu = 3.6$

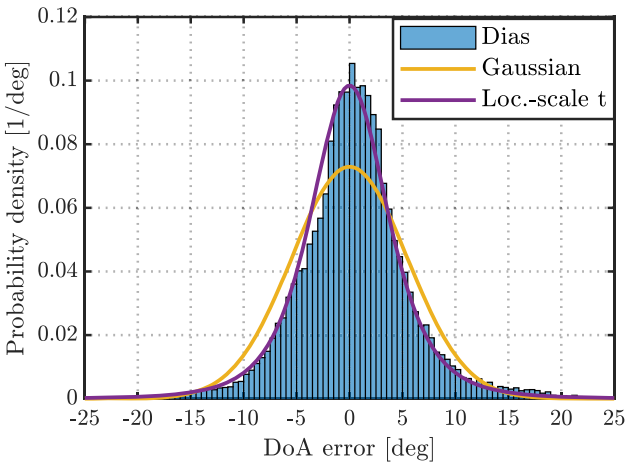

Fig. 17 Probability density histogram of the DoA estimation errors of the rover Dias, Gaussian pdf with $\mu = 0°, \sigma = 5.5°$ and Location-scale t pdf with $\mu = 0°, \sigma = 3.8°, \nu = 3.7$

Thus, we fit a zero-mean Gaussian distribution to the combined ranging errors of Dias and Vespucci, which yields $\sigma = 0.41\,\text{m}$. The Gaussian distribution is not a perfect fit for the given measurement data, but we consider it close enough to be used for algorithms which are restricted to Gaussian errors, e.g. the extended Kalman filter (EKF). To better represent the actual error characteristics, we fit a zero-mean location-scale t-distribution and obtain $\sigma = 0.28\,\text{m}, \nu = 3.6$. It has heavier tails than the Gaussian distribution, and thus better represents the actual ranging errors.

The DoA estimation error histogram for all signals received by the rover Dias is shown in Fig. 17. A very small amount of DoA estimation errors, 0.15%, are outside of the plotted range $[-25°, 25°]$. Again, their practical impact is usually small due to outlier rejection. Fitting a zero-mean Gaussian pdf gives $\sigma = 5.5°$. The Gaussian distribution does not represent the heavy-tailed nature of the DoA estimation error well. To better represent the actual error characteristics, we fit a location-scale t-distribution, which yields $\sigma = 3.8°$, $\nu = 3.7$.

Thus, we have shown that the ranging and DoA estimates can be modeled as the true range and DoA with additive noise following a location-scale t-distribution with the stated parameters.

7 Conclusion

In this paper, we have evaluated cooperative radio localization for robotic planetary exploration based on measurement data from a space-analogue mission executed on Mt Etna.

We found that the dominant error contributions for ranging and direction-ofarrival (DoA) observations are biases. These biases can be estimated and compensated during the mission by simultaneous localization and calibration (SLAC), which considerably improves ranging and DoA estimation accuracy. Consequently, SLAC also considerably improves the pose estimation accuracy compared to localization-only. For both SLAC and localization, cooperative outperform non-cooperative approaches. Furthermore, we identified the volcanic and ground metallic structures of the rovers and the lander as the cause for signal scattering and reflections.

Single-link localization, where a rover is connected to the network only via another rover, is shown to be feasible. Furthermore, we have shown that the ranging and DoA estimation errors can be modeled with a location-scale t-distribution. In conclusion, we have successfully demonstrated the feasibility and accuracy of cooperative radio localization for robotic planetary exploration with a space-analogue mission.

Author Contributions All authors contributed to the study conception and design. The hardware implementation was mainly done by Emanuel Staudinger and Robert Pöhlmann. The experiment was jointly conducted by all authors. The measurement data was analyzed by Robert Pöhlmann and the results were discussed with all authors. The first draft of the manuscript was written by Robert Pöhlmann and all authors commented on previous versions of the manuscript. All authors read and approved the final manuscript.

Funding Open Access funding enabled and organized by Projekt DEAL. This work was supported by the Helmholtz Association Project "Autonomous Robotic Networks to Help Modern Societies (ARCHES)" under Grant ZT-0033.

Declarations

Competing Interests The authors have no relevant financial or non-financial interests to disclose.

References

1. International Space Exploration Coordination Group: The Global Exploration Roadmap. https://www.globalspaceexploration.org
2. Schuster, M.J., Müller, M.G., Brunner, S.G., Lehner, H., Lehner, P., Sakagami, R., Dömel, A., Meyer, L., Vodermayer, B., Giubilato, R., Vayugundla, M., Reill, J., Steidle, F., von Bargen, I., Bussmann, K., Belder, R., Lutz, P., Stürzl, W., Smisek, M., Maier, M., Stoneman, S., Fonseca Prince, A., Rebele, B., Durner, M., Staudinger, E., Zhang, S., Pöhlmann, R., Bischoff, E., Braun, C., Schröder, S., Dietz, E., Frohmann, S., Börner, A., Hübers, H.-W., Foing, B., Triebel, R., Albu-Schäffer, A., Wedler, A., Roberts, J., Ishigami,

G.: The ARCHES space-analogue demonstration mission: Towards heterogeneous teams of autonomous robots for collaborative scientific sampling in planetary exploration. IEEE Robot. Autom. Lett. **5**(4), 5315–5322 (2020). https://doi.org/10.1109/LRA.2020.3007468
3. Kelly, A.: Mobile Robotics: Mathematics, Models, and Methods. Cambridge University Press, (2013)
4. Nister, D., Naroditsky, O., Bergen, J.: Visual odometry. In: Proc. 2004 IEEE Computer Society Conf. Computer Vision and Pattern Recognition, 2004. CVPR 2004., vol. 1, p. (2004). https://doi.org/10.1109/CVPR.2004.1315094
5. Cadena, C., Carlone, L., Carrillo, H., Latif, Y., Scaramuzza, D., Neira, J., Reid, I., Leonard, J.J.: Past, present, and future of simultaneous localization and mapping: Toward the robust-perception age. IEEE Trans. Robot. **32**(6), 1309–1332 (2016). https://doi.org/10.1109/TRO.2016.2624754
6. Schönfeldt, M., Grenier, A., Delépaut, A., Giordano, P., Swinden, R., Ventura-Traveset, J., Blonski, D., Hahn, J.: A system study about a lunar navigation satellite transmitter system. In: Proc. European Navigation Conf. (ENC), pp. 1–10 (2020). https://doi.org/10.23919/ENC48637.2020.9317521
7. ESA: Lunar Satellites. https://www.esa.int/Applications/Telecommunications_Integrated_Applications/Lunar_satellites Accessed 2022-02-08
8. Zhang, S., Pöhlmann, R., Staudinger, E., Dammann, A.: Assembling a swarm navigation system: Communication, localization, sensing and control. In: Proc. 1st IEEE Int. workshop communication and networking for swarms robotics (RoboCom) (2021). https://doi.org/10.1109/CCNC49032.2021.9369547
9. Patwari, N., Ash, J.N., Kyperountas, S., Hero, A.O., Moses, R.L., Correal, N.S.: Locating the nodes: Cooperative localization in wireless sensor networks. IEEE Signal Process. Mag. **22**(4), 54–69 (2005). https://doi.org/10.1109/MSP.2005.1458287
10. Sahinoglu, Z., Gezici, S., Güvenc, I.: Ultra-Wideband Positioning Systems: Theoretical Limits, Ranging Algorithms. Cambridge University Press, And Protocols (2011)
11. Viberg, M.: Introduction to array processing. In: Zoubir, A.M., Viberg, M., Chellappa, R., Theodoridis, S. (eds.) Array and Statistical Signal Processing. Academic Press Library in Signal Processing, vol. 3, pp. 463–502. Elsevier, (2014). Chap. 11. https://doi.org/10.1016/B978-0-12-411597-2.00011-4
12. Pöhlmann, R., Almasri, S.A., Zhang, S., Jost, T., Dammann, A., Hoeher, P.A.: On the potential of multi-mode antennas for direction-of-arrival estimation. IEEE Trans. Antennas Propag. **67**(5), 3374–3386 (2019). https://doi.org/10.1109/TAP.2019.2899010
13. Win, M.Z., Shen, Y., Dai, W.: A theoretical foundation of network localization and navigation. Proc. IEEE **106**(7), 1136–1165 (2018). https://doi.org/10.1109/JPROC.2018.2844553
14. Buehrer, R.M., Wymeersch, H., Vaghefi, R.M.: Collaborative sensor network localization: Algorithms and practical issues. Proc. IEEE **106**(6), 1089–1114 (2018). https://doi.org/10.1109/JPROC.2018.2829439
15. Kay, S.M.: Fundamentals of Statistical Signal Processing, Volume I: Estimation Theory, 1 edition edn. Prentice Hall, (1993)
16. Van Trees, H.L., Bell, K.L. (eds.): Bayesian Bounds for Parameter Estimation and Nonlinear Filtering/Tracking. IEEE Press, (2007)
17. Shen, Y., Win, M.Z.: Fundamental limits of wideband localization–Part I: A general framework. IEEE Trans. Inf. Theory **56**(10), 4956–4980 (2010). https://doi.org/10.1109/TIT.2010.2060110
18. Shen, Y., Wymeersch, H., Win, M.Z.: Fundamental limits of wideband localization–Part II: Cooperative networks. IEEE Trans. Inf. Theory **56**(10), 4981–5000 (2010). https://doi.org/10.1109/TIT.2010.2059720
19. Shen, Y., Win, M.: On the accuracy of localization systems using wideband antenna arrays. IEEE Trans. Commun. **58**(1), 270–280 (2010). https://doi.org/10.1109/TCOMM.2010.01.080141
20. Han, Y., Shen, Y., Zhang, X.-P., Win, M.Z., Meng, H.: Performance limits and geometric properties of array localization. IEEE Trans. Inf. Theory **62**(2), 1054–1075 (2016). https://doi.org/10.1109/TIT.2015.2511778
21. Pöhlmann, R., Zhang, S., Dammann, A., Hoeher, P.A.: Fundamental limits for joint relative position and orientation estimation with generic antennas. In: Proc. 26th European Signal Processing Conf. (EUSIPCO), Rome, Italy, pp. 697–701 (2018). https://doi.org/10.23919/EUSIPCO.2018.8553226
22. Wymeersch, H., Lien, J., Win, M.Z.: Cooperative localization in wireless networks. Proc. IEEE **97**(2), 427–450 (2009). https://doi.org/10.1109/JPROC.2008.2008853
23. Schloemann, J., Buehrer, R.M.: On the value of collaboration in location estimation. IEEE Trans. Veh. Technol. **65**(5), 3585–3596 (2016). https://doi.org/10.1109/TVT.2015.2442173
24. Bar-Shalom, Y., Li, X.R., Kirubarajan, T.: Estimation with Applications to Tracking and Navigation: Theory Algorithms and Software. John Wiley & Sons, (2004)
25. Peral-Rosado, J.A., Raulefs, R., López-Salcedo, J.A., Seco-Granados, G.: Survey of cellular mobile radio localization methods: From 1G to 5G. IEEE Commun. Surveys Tut. 20(2), 1124–1148 (Secondquarter 2018). https://doi.org/10.1109/COMST.2017.2785181
26. Bourdoux, A., Barreto, A.N., van Liempd, B., de Lima, C., Dardari, D., Belot, D., Lohan, E.-S., Seco-Granados, G., Sarieddeen, H., Wymeersch, H., Suutala, J., Saloranta, J., Guillaud, M., Isomursu, M., Valkama, M., Aziz, M.R.K., Berkvens, R., Sanguanpuak, T., Svensson, T., Miao, Y.: 6G white paper on localization and sensing (2020). arXiv:2006.01779 [cs, eess]
27. Zafari, F., Gkelias, A., Leung, K.K.: A survey of indoor localization systems and technologies. IEEE Commun. Surveys Tuts. **21**(3), 2568–2599 (2019). https://doi.org/10.1109/COMST.2019.2911558
28. Luo, Y., Law, C.L.: Indoor positioning using UWB-IR signals in the presence of dense multipath with path overlapping. IEEE Trans. Wireless Commun. **11**(10), 3734–3743 (2012). https://doi.org/10.1109/TWC.2012.081612.120045
29. Conti, A., Guerra, M., Dardari, D., Decarli, N., Win, M.Z.: Network experimentation for cooperative localization. IEEE J. Sel. Areas Commun. **30**(2), 467–475 (2012). https://doi.org/10.1109/JSAC.2012.120227
30. Pöhlmann, R., Staudinger, E., Zhang, S., Dammann, A.: Simultaneous localization and calibration for radio navigation on the Moon: Results from an analogue mission. In: Proc. ION GNSS+ 2022, Denver (2022). https://doi.org/10.33012/2022.18557
31. Pöhlmann, R., Staudinger, E., Zhang, S., Broghammer, F., Dammann, A., Hoeher, P.A.: Cooperative radio navigation for robotic exploration: Evaluation of a space-analogue mission. In: Proc. IEEE/ION Position, Location and Navigation Symp. (PLANS), pp. 372–380 (2023). https://doi.org/10.1109/PLANS53410.2023.10140026
32. Staudinger, E., Zhang, S., Pöhlmann, R., Dammann, A.: The role of time in a robotic swarm: A joint view on communications, localization, and sensing. IEEE Commun. Mag. **59**(2), 98–104 (2021). https://doi.org/10.1109/MCOM.001.2000593
33. Pöhlmann, R., Zhang, S., Staudinger, E., Dammann, A., Hoeher, P.A.: Simultaneous localization and calibration for cooperative radio navigation. IEEE Trans. Wireless Commun. **21**(8), 6195–6210 (2022). https://doi.org/10.1109/TWC.2022.3147671
34. Helmholtz Future Topic Project ARCHES (Autonomous Robotic Networks to Help Modern Societies). https://www.arches-projekt.de/en/helmholtz-future-topic-project-arches/

35. Staudinger, E.: Round-trip delay ranging with orthogonal frequency division multiplex signals. PhD thesis, Fachbereich für Physik und Elektrotechnik, Universität Bremen (2015)
36. Rappaport, T.S.: Wireless Communications: Principles And Practice. Prentice Hall, (2002)
37. Kaplan, E.D., Hegarty, C.J. (eds.): Understanding GPS: Principles and Applications, 2nd edn. Artech House Mobile Communications, Artech House (2006)
38. Morton, Y.J., Van Diggelen, F.S.T., Spilker, J.J., Parkinson, B.W., Lo, S.C., Gao, G.X. (eds.): Position, Navigation, and Timing Technologies in the 21st Century: Integrated Satellite Navigation, Sensor Systems, and Civil Applications vol. 1. John Wiley & Sons, (2021)
39. Staudinger, E., Pöhlmann, R., Dammann, A., Zhang, S.: Limits on cooperative positioning for a robotic swarm with time of flight ranging over two-ray ground reflection channel. Electronics **12**(9), 2139 (2023). https://doi.org/10.3390/electronics12092139
40. Costa, M., Koivunen, V., Viberg, M.: Array processing in the face of nonidealities. In: Zoubir, A.M., Viberg, M., Chellappa, R., Theodoridis, S. (eds.) Academic Press Library in Signal Processing. Academic Press Library in Signal Processing, vol. 3, pp. 819–857. Elsevier, (2014). https://doi.org/10.1016/B978-0-12-411597-2.00019-9
41. Pöhlmann, R., Zhang, S., Staudinger, E., Caizzone, S., Dammann, A., Hoeher, P.A.: Bayesian in-situ calibration of multiport antennas for DoA estimation: Theory and measurements. IEEE Access **10**, 37967–37983 (2022). https://doi.org/10.1109/ACCESS.2022.3164520
42. Schuster, M.J., Brunner, S.G., Bussmann, K., Büttner, S., Dömel, A., Hellerer, M., Lehner, H., Lehner, P., Porges, O., Reill, J., Riedel, S., Vayugundla, M., Vodermayer, B., Bodenmüller, T., Brand, C., Friedl, W., Grixa, I., Hirschmüller, H., Kaßecker, M., Márton, Z.-C., Nissler, C., Ruess, F., Suppa, M., Wedler, A.: Towards autonomous planetary exploration: The Lightweight Rover Unit (LRU), its success in the SpaceBotCamp challenge, and beyond. Journal of Intelligent & Robotic Systems **93**(3–4), 461–494 (2019). https://doi.org/10.1007/s10846-017-0680-9
43. Fleury, B.H., Tschudin, M., Heddergott, R., Dahlhaus, D., Pedersen, K.I.: Channel parameter estimation in mobile radio environments using the SAGE algorithm. IEEE J. Sel. Areas Commun. **17**(3), 434–450 (1999). https://doi.org/10.1109/49.753729
44. Antreich, F., Nossek, J.A., Utschick, W.: Maximum likelihood delay estimation in a navigation receiver for aeronautical applications. Aerosp. Sci. Technol. **12**(3), 256–267 (2008). https://doi.org/10.1016/j.ast.2007.06.005
45. Walter, M., Shutin, D., Fiebig, U.-C.: Delay-dependent Doppler probability density functions for vehicle-to-vehicle scatter channels. IEEE Trans. Antennas Propag. **62**(4), 2238–2249 (2014). https://doi.org/10.1109/TAP.2014.2301432
46. Guerra, A., Guidi, F., Dardari, D.: Single-anchor localization and orientation performance limits using massive arrays: MIMO vs. beamforming. IEEE Trans. Wireless Commun. 17(8), 5241–5255 (2018). https://doi.org/10.1109/TWC.2018.2840136
47. Abu-Shaban, Z., Wymeersch, H., Abhayapala, T., Seco-Granados, G.: Single-anchor two-way localization bounds for 5G mmWave systems. IEEE Trans. Veh. Technol. **69**(6), 6388–6400 (2020). https://doi.org/10.1109/TVT.2020.2987039

Robert Pöhlmann received the B.Sc. and M.Sc. degrees in electrical engineering and information technology from the Technical University of Munich (TUM) in 2014 and 2016, respectively. He then joined the Institute of Communications and Navigation, German Aerospace Center (DLR) as a Research Staff Member. In 2022, he received the Ph.D. with distinction from the Kiel University. He is a recipient of the VDE ITG dissertation award 2023. His current research interests include cooperative and hybrid localization as well as statistical signal processing for multi-antenna systems.

Emanuel Staudinger received the M.Sc. degree in Embedded Systems Design from the University of Applied Sciences of Hagenberg, Austria, in 2010. Since 2010, he is with the Institute of Communications and Navigation of the German Aerospace Center (DLR), Wessling, Germany. He received a Ph.D. with distinction from the Institute of Electrodynamics and Microelectronics at the University of Bremen, Germany, in 2015. His current research interests include system design for cooperative positioning, experimental platform design based on SDRs, and experimental validation for swarm navigation.

Siwei Zhang received his B.Sc. in electrical engineering from Zhejiang University, China, in 2009, his M.Sc. in communication engineering from the Technical University of Munich, Germany, in 2011, and his Dr.-Ing. (Ph.D.) in electrical engineering from the University of Kiel, Germany, in 2020. In 2012, he joined the Institute of Communications and Navigation of the German Aerospace Center (DLR) as a research staff member. His research interests lie in statistical signal processing in wireless communication and navigation, particularly in multi-agent joint communication, navigation and sensing. He is a recipient of the 2021 DLR Science Award.

Armin Dammann received the Dipl.- Ing. (M.Sc.) and Dr.-Ing. (Ph.D.) degrees in Electrical Engineering from the University of Ulm, Germany, in 1997 and 2005 respectively. In 1997 he joined the Institute of Communications and Navigation of the German Aerospace Center (DLR) as a research staff member. Since 2005 he is head of the Mobile Radio Transmission Re-search Group. His research interest and activities include signal design and signal processing for terrestrial wireless communication and navigation systems. In these fields, he has been active in several EU-projects, e.g., WINNER, WHERE and WHERE2. Armin Dammann is lecturer at the Technical University of Munich for Robot and Swarm Navigation.